# Methacrylic Acid Polymerization. Travelling Waves Observed by Nuclear Magnetic Resonance Imaging

**Bruce J. Balcom, T. Adrian Carpenter, and Laurance D. Hall***

*Herchel Smith Laboratory for Medicinal Chemistry, University of Cambridge School of Clinical Medicine, Cambridge CB2 2PZ, U.K.*

*Received June 8, 1992; Revised Manuscript Received August 31, 1992*

ABSTRACT: Nuclear magnetic resonance imaging (NMRI) has been used to examine travelling waves of benzoyl peroxide initiated methacrylic acid polymerization. The polymer/monomer interface is sharply defined (<1.2 mm) and is characterized by an abrupt discontinuity in the NMR spin–spin relaxation time constant ($T_2$). The front velocity measured from a series of one-dimensional magnetization profiles is 0.61 cm/min. The polarizing magnetic field $\mathbf{B}_0$ has little or no effect on the observed velocity.

## Introduction

Nuclear magnetic resonance imaging (NMRI) has attracted interest recently through its application to material science and other nonmedical fields.[1-5] As part of a continuing effort in this field we now report the application of NMRI to the recently discovered autocatalytic polymerization of methacrylic acid.[6] An autocatalytic reaction in an unstirred vessel can support a constant velocity wave front which results from the coupling of molecular diffusion to chemical reaction. Numerous reactions in solution have been described in which a reaction front propagates through the medium from the site of an initial perturbation.[7-13] Moving fronts, which manifest themselves in some physicochemical discontinuity are ideal systems for examination by NMRI and have been the subject of several recent reports.[14-17]

In the present study the discontinuity observed by NMRI is the drastic decrease in the NMR spin–spin relaxation time constant ($T_2$), of proton resonances which occurs upon polymerization of an organic compound.[18] The goals are 3-fold: (1) to examine the qualitative behavior of the methacrylic system before and after the travelling wave is established; (2) to examine analytically the shape and structure of the wavefront (with a microscopic technique such as NMRI it is possible to examine the wave for significant structure in both the monomer, polymer, and interfacial zones; Pojman, in the original paper, was able to observe the wavefront solely by eye[6]); (3) to determine whether the magnetic field $\mathbf{B}_0$ has a measurable effect on the kinetics of reaction. Free radical polymerization has recently been investigated by NMRI,[18,19] but there is ample precedent in the literature for the kinetics of such reactions to be altered by the presence of a magnetic field.[20] Unfortunately, the sensitivity of NMRI to a large number of image contrast generating mechanisms in many cases precludes observation of a direct relationship between observed signal intensity and concentration of material. Therefore kinetic rate constants are difficult to establish. The methacrylic acid reaction is autocatalytic because an exothermic free radical polymerization is coupled to the thermal decomposition of the initiator, benzoyl peroxide. If $\mathbf{B}_0$ alters the kinetics of reaction, the resultant change in the rate of heat production will manifest itself as a change in the wave velocity and thereby provide a clear, albeit indirect, measure of any possible $\mathbf{B}_0$ effect.

## Experimental Section

Methacrylic acid (Aldrich, 99%) was used without purification; the large excess initiator, benzoyl peroxide (Aldrich, 25% water), quickly exhausts the inhibitor (1000 ppm hydroquinone, 250 ppm hydroquinone momomethyl ether). *N,N*-Dimethylaniline (Aldrich, 99%) was used as the accelerator, and 1,4-dibromotetrafluorobenzene (Aldrich, 99%) was used as a heteronuclear NMR tracer.

Reactions were started by adding $^1/_2$ mL of dimethylaniline to the top of 24–27 mL of methacrylic acid containing dissolved benzoyl peroxide (0.88 g/80 mL). All experiments began at room temperature, 20–22 °C. Measurements (visual, temperature, or NMR) commenced within 1 min of aniline addition.

The reaction chamber comprised an 8-dram glass sample vial (height 9.6 cm, diameter 2.3 cm), surrounded by a thin (0.5 mm), flexible Teflon sheet, snugly inserted into a closed-bottom transparent Perspex cylinder of inner diameter 2.59 cm and height 10 cm. The Teflon sheet and Perspex cylinder act in part as thermal insulation which is vital to maintain the viability of the relatively slow moving front observed in these experiments. Systems with higher velocities (more initiator) were not measured due to the technical difficulties associated with a large heat flux—induced breakage of the glass reaction chamber. A small gap in the Teflon sheet permitted visual examination of the advancing polymer front as required. Temperature measurements were made with a calibrated type T thermocouple (Radio Spares, UK); the leads of the thermocouple were fixed midway down the inner side of the glass vessel with Araldite epoxy (Ciba-Geigy), and the probe tip was bent so that it measured the temperature in the center of the sample vial.

NMR measurements were performed with an Oxford Research Systems Biospec 1 instrument controlled by an Aspect 3000 computer, with a 2-T Oxford Instruments horizontal bore (31-cm) magnet and a home-built gradient set. The $^1$H and $^{19}$F resonance frequencies of this system were 83.7 and 78.9 MHz, respectively. The sample vials were held vertically by a polystyrene collar and positioned inside a modified split ring resonator NMR probe[21] (6.3-cm diameter, height 11 cm) which was tunable to either the $^1$H or $^{19}$F frequencies. Broad-band radio-frequency excitation pulses were used for both $^1$H and $^{19}$F (90° pulse, 60 $\mu$s). For $^1$H experiments, a magnetic field gradient of 6000 Hz/cm, oriented parallel to the long axis of the sample gave a field of view of 10.4 cm with a nominal pixel resolution of 0.4 mm; echo times ($T_e$) were 8.25 and 56 ms (spectral width 62 500 Hz). For $^{19}$F experiments, a magnetic field gradient of 940 Hz/cm gave a 10.6-cm field of view with a nominal pixel resolution of 0.4 mm; echo times, $T_e$, were 30 ms with a spectral width of 10 000 Hz. In all cases 256 complex time domain data points were collected for each of 256 profiles, that were collected every 5 s.

The imaging sequence used was a standard one-dimensional 90°–$T_e$/2–180°–$T_e$/2–acquire spin echo sequence. Experimental echo times were kept much shorter than the characteristic time for the front to move by one pixel; hence the profiles acquired may be considered "snapshots" of the dynamic system as it evolves.

## Results

The NMRI imaging sequence is optimized for detection of the spatial variation of $T_2$. The formula for the signal

0024-9297/92/2225-6818$03.00/0 

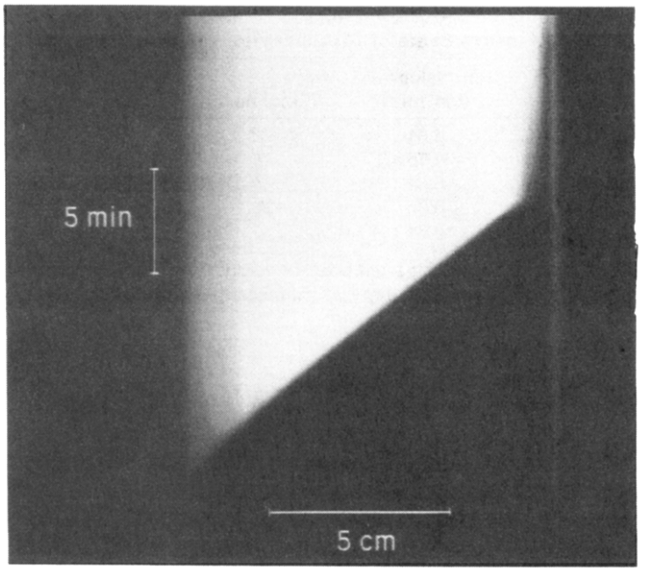


**Figure 1.** Short echo time, $T_e$ = 8.25 ms, data for methacrylic acid. The image is formed from 256 profiles acquired at 5-s intervals. Scale bars indicate the sample size and the time course of the travelling front. The polymer in this image has low signal intensity; the monomer has high intensity. The sharp drop from high to low signal intensity is characteristic of the reaction front. The induction period is 8 min.

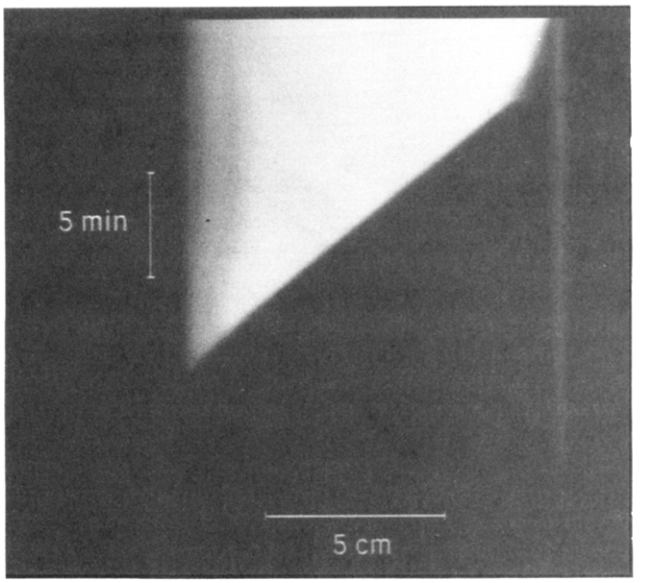


**Figure 2.** Short echo time experiment as per Figure 1 but with an induction period of 4 min. Note the fizzled ignition partway through the induction period.

intensity detected at a point for this sequence is given by eq 1, where $\rho$ is the nuclear density, $T_2$ is the spin–spin

$$S = \rho \exp(-T_e/T_2)(1 - \exp(-T_R/T_1)) \quad (1)$$

nuclear relaxation time, and $T_1$ is the spin–lattice relaxation time. All three of these variables are characteristic of the physical state of the system under study.[1,22,23] The variables $T_e$ and $T_R$ are parameters which determine the overall timing of the imaging sequence. The echo time $T_e$ is twice the delay between the 90 and 180° pulses, and $T_R$ is the delay between successive 90° pulses. The delays used, long $T_R$ and short but variable $T_e$, were selected to optimize image contrast determined by the characteristic time $T_2$ in the second term of eq 1. The $T_2$ relaxation time is very sensitive to local motion of the nuclei under study.[22,23] Generally, freely mobile molecules, with short correlation times, have long $T_2$ values while motionally restricted or immobile molecules have very long correlation times and short $T_2$ values. Thus formation of a polymer from monomeric precursor leads to a characteristic change in local motion which will induce a marked drop in $T_2$ as the polymer is formed.[18] The $T_1$ relaxation times of monomeric methacrylic acid range between 1 and 2 s; a pulse repetition time ($T_R$) of 5 s will thus lead to partial saturation of the monomer signal. Spin–lattice relaxation times of polymers tend to be less than 1 s,[23,24] and so partial saturation is less significant for the polymer. Hence, by running experiments at a fixed repetition rate and varying the echo time, the $T_1$ effects will normalize out and a true $T_2$ effect should be observed.

Figures 1 and 2 are typical polymerization images, displayed as profile intensity (horizontal dimension) as a function of time (vertical dimension). They show an initially uniform distribution of monomer solution of high signal intensity, with a narrow band of aniline showing as a bright spot at the top of the reaction vessel (right side of each profile). Qualitatively, one observes an induction period, of variable duration, where the polymer front (reflected by short $T_2$ values) slowly proceeds down the sample vial. After the induction period (Table I) the reaction suddenly accelerates and enough heat is produced to cause the existing polymer to expand upward, thereby producing the dislocation of the aniline signal noted in Figure 1. Initially, the reaction front, represented by the discontinuity in signal intensity, moves forward rapidly but then settles into a constant-velocity wave which propagates through the rest of the methacrylic acid solution.

**Table I**
**NMRI Measurements of Methacrylic Acid Polymerization**

| exp no. | $T_e$ (msc) | induction period[a] (min) | front velocity[b] (cm/min) |
|---|---|---|---|
| 1 | 8.25 | 8 | 0.61 |
| 2 | 56 | 4 | 0.62 |
| 3 | 56 | 5 | 0.60 |
| 4 | 8.25 | 4 | 0.60 |
| 5 | 30[c,d] | 14 | 0.59 |
| 6 | 30[c,d] | 3 | 0.63 |
| 7 | 8.25[c] | 8 | 0.55 |
| 8 | 8.25 | 4 | 0.60 |
| 9 | 46 | [e] | 0.68 |

[a] Estimated from the image including time before acquisition commenced. [b] Measured after the induction period. [c] 4% 1,4-dibromotetrafluorobenzene by weight. [d] $^{19}F$ measurement. [e] Propagation commenced before acquisition.

A plot of the interface position, observed in Figure 1, as a function of time yields a measure of the front velocity. The interface position is best estimated by the point of maximum change in slope (greatest increase in signal per unit length); a simple difference approximation to the derivative yields this point.[25] The plot (Figure 3a) is linear, as expected from Figure 1, and after linear regression gives a measure of the front velocity, 0.61 cm/min; the experimental uncertainty in this velocity (less than 1%) is much less than the spread in the measurements from all the NMRI experiments reported in Table I.

$^1H$ experiments with long echo times qualitatively resemble Figures 1 and 2, except with overall lower signal intensities. Because of the longer $T_e$, aniline partially immobilized in polymer is not visible in these images. The front velocity is measured as described above, and the results reported in Table I yield a mean velocity of 0.61 cm/min with a standard error of 0.01 cm/min. The $^1H$ experiments provide a direct measure of the behavior of

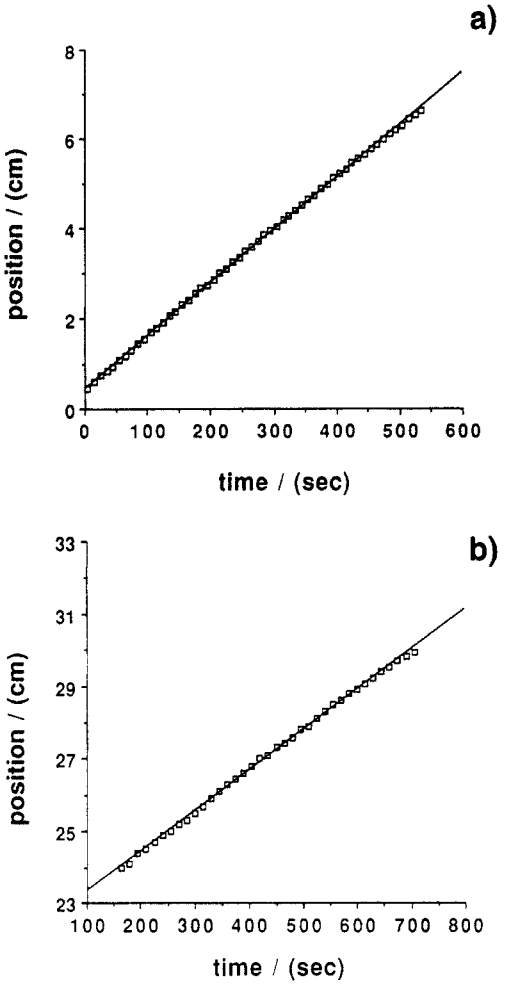


**Figure 3.** (a) Plot of the position of the monomer/polymer interface, determined from an NMRI experiment, as a function of time after the induction period. For clarity only every second data point is shown. The front velocity is 0.61 cm/min. (b) Plot of the monomer/polymer interface, determined optically, as a function of time after aniline is added. The measurement was made external to the magnet and gave a front velocity of 0.61 cm/min.

the constituent parts of the polymer network. Companion experiments with a $^{19}F$ tracer were undertaken, in part (vide infra), to provide a means of observing a purely environmental effect, i.e., the effect of the nascent polymer on the surrounding solution. The added tracer (4% on a weight basis) appears to have little or no effect on the measured velocity (including the case where the $^{1}H$ signal was measured in the presence of the tracer). (The polymer wave, once initiated, has also been observed to propagate through close-packed slica gel in a methacrylic acid/benzoyl peroxide solution.) Once more the images (not shown) qualitatively resemble Figures 1 and 2, but with two major differences: (1) the signal-to-noise is much poorer because of the lower nuclear density of the $^{19}F$ nuclei, and (2) the aniline signal is not observed.

Measurements of the front velocity and of temperature variation about the front were also performed in the laboratory. The front is visible to an external observer as a sharp discontinuity between white polymer mass and clear monomer-rich solution.[6] The slope of a plot of the front position, measured by a ruler fixed next to the backlit apparatus, as a function of time yields the wave velocity as shown in Figure 3b; the measured velocity in Figure 3b is 0.61 cm/min. The results of nine such measurements are given in Table II, and once again the uncertainty in any individual measurement is much less than the variation between experiments; the mean velocity is 0.64 cm/min,

**Table II**
**Optical Measurements of Methacrylic Acid Polymerization**

| exp no. | front velocity[a,b] (cm/min) | exp no. | front velocity[a,b] (cm/min) |
|---|---|---|---|
| 1 | 0.61 | 6 | 0.64 |
| 2 | 0.70 | 7[c] | 0.63 |
| 3 | 0.64 | 8[c] | 0.64 |
| 4 | 0.65 | 9[c] | 0.67 |
| 5 | 0.64 | | |

[a] Measured by plotting front position versus time. [b] Measured after the induction period. [c] Temperature measured simultaneously.

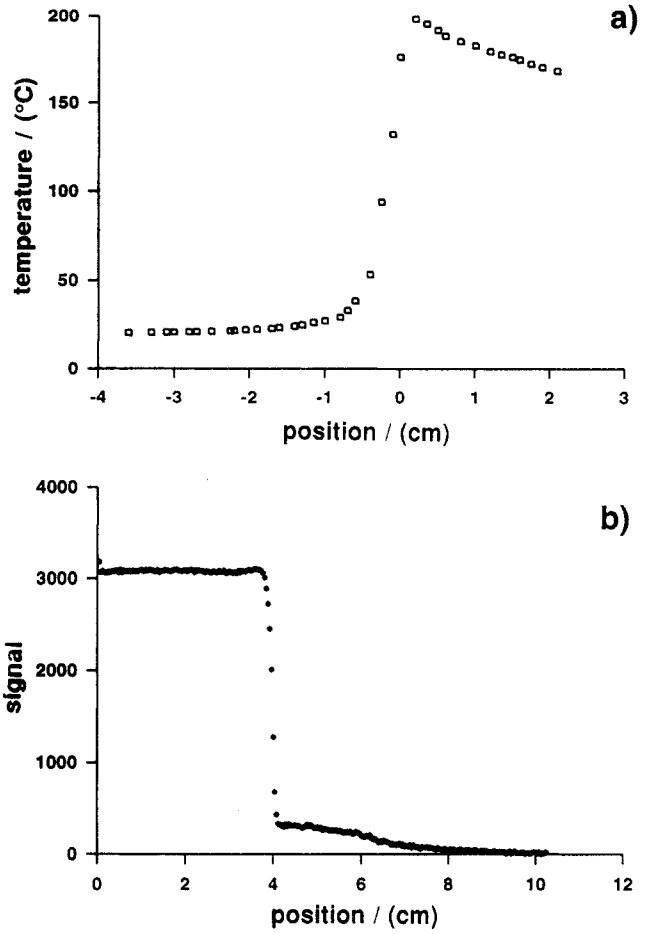


**Figure 4.** (a) Temperature variation near the reaction front. The drop in temperature after the reaction front is due to heat loss in the system. The temperature at the reaction front is 176 °C. (b) Signal variation of a point as a function of time based on a profile taken from Figure 1. $^{1}H$ short echo time experiment, $T_e$ = 8.25 ms.

with a standard error of 0.01 cm/min. In three of those measurements the temperature evolution of a point in solution was simultaneously measured, via a thermocouple, as the polymer wave approached and engulfed it. The temperature plot as a function of time was processed, via the measured velocity of the wave, to give a temperature map of the wave front and neighboring regions,[6] and a representative plot is reproduced as Figure 4a. The presence of the thermocouple does not alter the observed velocity.

## Discussion

We focus first on the qualitative aspects of the experiment. Clearly, it is possible both to observe and quantify the rate of polymer propagation through solution. As expected, this rate is constant (after the induction period) and the associated changes in $T_2$, the spin–spin relaxation time constant, provide a ready means of image contrast.

The rate measured in the magnet, 0.61 cm/min, is slightly less than the recent measurements of Pojman[6] at a comparable initiator concentration.

The structure of the induction period is perhaps the most significant qualitative feature of the experiment. Optically, the induction period appears to be quiescent; a mass of white polymer of somewhat indeterminate length forms but does not appear to change greatly until the ignition point when propagation begins. Figures 1 and 2 clearly show a polymer wave of some description proceeds from the aniline band, but the velocity is low and, as seen in these and other images, the front itself can be both discontinuous and of ragged appearance. The length of the induction period determined by NMRI may be as long as 14 min and appears to be related to the vigor with which aniline is added to the system. Rapid addition apparently leads to greater interfacial mixing and hence a decreased induction period. The experiments shown in Figures 1 and 2 illustrate this observation. In the first experiment (Figure 1) slow addition of aniline led to a long induction period with a smooth change in signal with position. In the second experiment (Figure 2) aniline was added more vigorously and one observes a faster rate of front movement during the induction period and at least one fizzled ignition. In this case the overall duration of the induction period is 4 min compared to 8 min for the experiment in Figure 1.

As discussed previously, one motivation for this work was to determine if a significant magnetic field effect exists for this particular reaction. The mechanism for such an effect would originate in the singlet state radical pair which is produced upon dissociation of the initiator peroxide bond. The putative effect is an indirect one since it is kinetic; not thermodynamic, in origin.[26] The efficiency of the initiation step is crucially dependent on the rate of cage recombination, which is the rate at which a newly-separated radical pair will recombine rather than initiate the reaction.[27] At high magnetic fields, $\mathbf{B}_o$ is predicted to inhibit the transformation of the singlet radical pair to a triplet state by decoupling the $T_+$ and $T_-$ states from $S_o$.[26] A triplet radical pair cannot recombine to form a chemical bond; the magnetic field decreases the likelihood that some radical pairs will enter a triplet state and thereby increases the rate of cage recombination. A decrease in the efficiency of the initiation step decreases the overall reaction rate. This effect will be particularly important in a high-viscosity medium where the rate of cage recombination is high.[28] This is precisely the situation either in the travelling-wave experiment or in the autoacceleration phase of a bulk free radical polymerization where the reaction takes place in a high-viscosity medium. Of vital interest, therefore, is both the dependence of the rate of reaction upon the initiation rate constant ($k_i$) and the dependence of the front velocity on the rate of heat production. Elementary free radical kinetics tell us that the rate of reaction, and therefore the rate of heat production, is proportional to the square root of $k_i$.[29]

Flame theory[30,31] closely models many aspects of the polymer front behavior observed and may be used to predict the dependence of the front velocity on the rate of reaction. In essence it treats a complex chemical reaction as a single exothermic reaction step with a large activation energy. The reaction at a point in space generates a large thermal gradient which can overcome the activation energy of the system at a neighboring point and lead to linear propagation of the flame front. This is also the behavior of the polymer front system; however, one should note the front velocity is much less than typically observed for flames.[30,31] The front velocity is diminished, in part, because the thermal diffusivity of methacrylic acid is much less than the thermal diffusivity of a gas. Flame theory predicts a front velocity which is proportional to the square root of the reaction rate.[30,31] When this theory is assumed applicable, a large applied $\mathbf{B}_o$ should result in a decreased velocity, but a 50% change in the initiation rate, other things being equal, will only result in a 10% decrease in the front velocity. Therefore the front velocity does not, as one might hope, amplify the effect of small changes early in the chain reaction; however, it should still be sensitive to very gross alterations in the rate of initiation. A statistical comparison (unpaired t test, 2% confidence level) of the results in Tables I and II shows no significant difference in the mean values of 0.61 and 0.64 cm/min measured in and out of the magnetic field, respectively. At a 5% confidence level, however, the values are statistically different. Therefore we may conclude that a measurable magnetic field effect on the travelling-wave reaction may exist but is not yet established. If it does exist, it certainly has a minor effect on the front velocity. Similarly, a magnetic field effect on other thermally induced free radical polymerization reactions is possible but, through the square root dependence on the initiation rate, is unlikely to lead to large alterations in the reaction rate.

The final aim of this work was to examine the structure of the polymer front and the neighboring regions of space. Via profiles acquired with different experimental delays and using both $^1$H and $^{19}$F nuclei, our intent was to make quantitative statements about the breadth of the reaction zone with a particular emphasis on determining the molecular processes in the vicinity of the moving front. Two factors prevent direct examination of the signal variation within any given spatial profile. (1) The probe response is nonuniform over the length of the sample. (2) A quadrature error in the phase-sensitive detection of the NMR signal[32] gives a Fourier-transformed profile where some of the signal from the intense left-hand side (monomer) of the profile is reflected about a point and observed as a low-intensity mirror image superimposed on the signal from the polymer region of the sample. Although both these factors obscure detail in regions of space which follow the polymer wave, they do not preclude detection and tracking of the front discussed earlier. Examining profiles along the time axis of images analogous to Figures 1 and 2 normalizes spatial variation in probe response and simultaneously avoids the reflected intensity artifact. (A time axis profile from the right-hand one-quarter of the image still has the reflected intensity artifact superimposed on the low-intensity polymer signal.) This examination of the variation in signal from a point in space as a function of time as the polymer wave approaches is directly analagous to the procedure whereby the temperature variation about the reaction front was mapped (Figure 4a). This approach presumes that the reaction front, over the region of linear propagation is self-similar, or is in a quasi steady state with a moving coordinate system, and is an assumption commonly used in analyzing travelling-wave systems.[33] Examination of a variety of profiles along both the time and space axes shows the front is indeed self-similar. Figure 4b shows a time profile (vertical dimension in Figure 1) of a short-$T_e$ (8.25-ms) $^1$H experiment; Figure 5a shows a similar time profile from a long-$T_e$ (56-ms) experiment. For comparison Figure 5b shows a time profile of the signal intensity from a $^{19}$F experiment. The resolution in each time profile is the

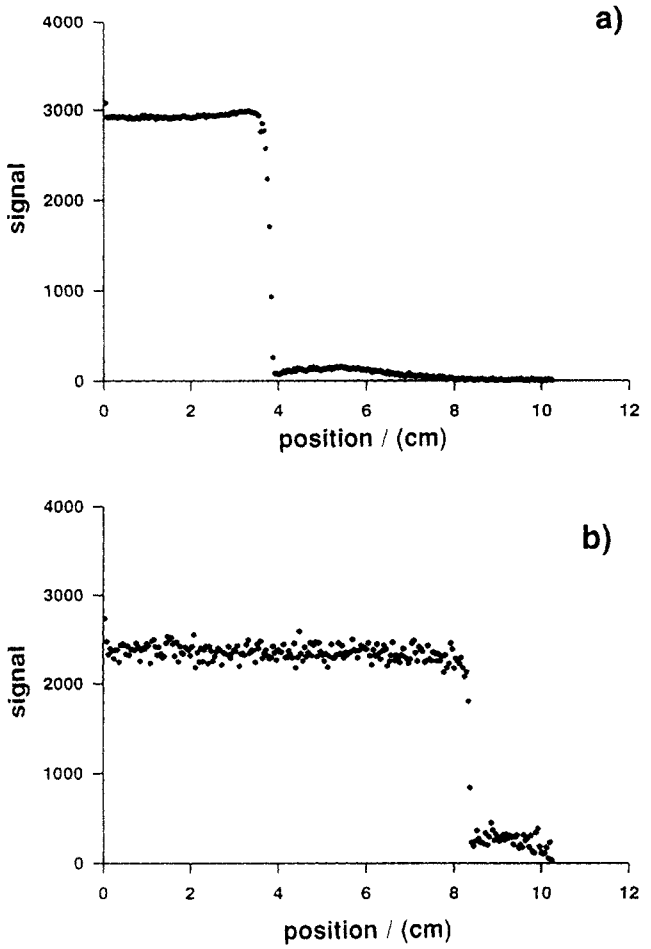


**Figure 5.** (a) Signal variation of a point as a function of time from a representative $^1H$ long echo time experiment, $T_e = 56$ ms. (b) Signal variation of a point as a function of time from a representative $^{19}F$ experiment.

increment between profiles (5 s) which may be converted to a distance measurement via the measured front velocity.

The sharp drop in intensity observed in all three profiles marks the point at which the polymer front engulfs that point in solution. Immediately prior to this transition there is little observable structure. There may be a slight increase in Figures 4b and 5a immediately preceding the wave but it varies from profile to profile and experiment to experiment. A priori, one might have expected some manifestation of the large temperature increase (Figure 4a) which preceeds the polymer front. No such effect is observed because the increase in mobility of the liquid monomer with temperature, and hence of $T_2$, is unobservable over the scale of $T_2$ values which are discriminated by echo times of under 100 ms. However, two competing processes do occur, a decrease in correlation time and thereby increased $T_2$, which is opposed by the sudden onslaught of reaction which freezes molecular motion in a rigid, although hot, polymer matrix. Correlation times are therefore longer and $T_2$ shorter, which we observe as a decrease in signal intensity.

The breadth of the transition in Figures 4b and 5a is approximately 10 pixels, or 4 mm (via the front velocity). Long echo time experiments should detect partial polymerization over a greater distance than is observable in a short echo time experiment. No difference is noted between these two measurements which suggests that the transition zone observed by each is identically 4 mm. There is, however, a complication in the interpretation due to the chemical shift dispersion effects of the methacrylic acid spectrum which has four singlets (scalar coupling is approximately 1 Hz and therefore not resolvable) that resonate at 12.3 ppm (singlet, acid proton) 6.2 and 5.6 ppm (vinyl protons), and 2 ppm (singlet, methyl group). Although the transmitter radio frequency is set at the frequency of the high-field vinyl proton resonance, the frequency difference of the other resonances is enough to cause signal leakage over the three or four neighboring pixels mapped by the field gradient.[34] The observed transition is therefore artificially broadened by this chemical shift dispersion and is likely 3 or 4 times sharper than observed. Although the $^{19}F$ profiles are quite noisy compared to the $^1H$ profiles, the transition between free and polymer-bound molecules is clearly discernable. By design, the $^{19}F$ tracer employed has four fluorine atoms which are all magnetically equivalent and therefore no chemical shift dispersion exists. The transition observed experimentally is two or three pixels wide which with a pixel resolution of 5 s (converted via the front velocity) yields a transition of 1.2 mm. This observed width is so narrow that it may be used only as an upper limit on the true width of the reaction zone. A slight misalignment of the sample with the applied gradient, or a minor spatial variation in reaction front, would broaden the observed width. It appears, therefore, that the reaction front moves through solution approximating a step function where the reaction zone is effectively a $\delta$ function.

Immediately following the transition region, the $^1H$ profiles show a somewhat unexpected plateau in signal intensity (for long $T_e$ an increase before a plateau) which is followed by a slow fall in intensity. Although the decrease in signal intensity between the monomer and polymer is precipitous, it is found that the signal-to-noise ratio is still good in the region immediately behind the reaction front (even for long $T_e$). This signal could be from residual monomer sequestered in the hot polymer. It is a common feature of bulk polymerization that up to 10% of monomer may remain unpolymerized due to the steep drop in initiator efficiency as the viscosity increases.[28] Hence the observation that monomer remains in the sample is not unexpected and is supported by the strong smell of methacrylic acid which lingers after a cooled polymer rod is broken open several days after an experiment. The ratio of the signal intensities for both the long and short echo profiles 1.5 cm away from the transition should depend only on the ratio of eq 1 for the two experiments with different $T_e$ values. On the basis of that comparison, $T_2$ may be estimated at 75 ms. This is very long for a polymer even above its glass transition temperature.[23,24] The glass transition temperature of poly(methacrylic acid)[35] is not commonly reported: however, a Russian group has estimated a $T_g$ of 228 °C.[36] Therefore it appears likely that the residual signal intensity in Figures 6 and 7 originates with residual monomer trapped in polymer once the reaction front has passed.

As expected the difference in signal between Figures 4b and 5a is very small in the monomer region, which confirms that the $T_2$ of the bulk monomer is very long, certainly much greater than 58 ms. The slow decrease in signal with time after the plateau in the polymer almost certainly reflects the decrease in motional averaging of the small methacrylic acid monomers or oligomers as the polymer cools (Figure 5a). A similar effect is observed in Figure 1 where the aniline signal dies out as the polymer cools. The aniline signal persists as long as it does in Figure 1 because the aniline mole fraction is very high and polymer formation is therefore much less effective in restricting motion.

The discrepancy in the shape of the plateau region for long and short echo time experiments is more difficult to explain. Note, however, that the extent of these regions, 1.5–2 cm, corresponds in Figure 4a to the distance from the reaction front where the temperature is above the normal boiling point of bulk methacrylic acid. Motional averaging would be expected to be very effective in this region and should lead to prolonged signal over a significant temperature regime (>160 °C). However, profiles measured at long $T_e$ indicate a decreased $T_2$ close to the reaction front. The effect is a minor one but is reproducible from experiment to experiment and profile to profile. The inevitable exhaustion of the initiator near the temperature maximum and the decline in temperature over this depressed region suggest that the reaction is complete in this area of space. Therefore, we speculate that the weak signal near the polymer front in a long echo time experiment originates from a temperature/phase effect. Further work is necessary to fully understand this feature of the experiment. The most useful control experiment would be to heat the cooled polymer after reaction in order to observe signal intensity, or $T_2$, as a function of temperature. Although this experiment would discriminate between a temperature/phase effect and any effect due to the proximity of the reaction front, it would be difficult to achieve the very high temperatures generated by the reaction, which approach 200 °C.

## Conclusion

In this study NMRI has proven to be a valuable analytical tool in unravelling the behavior of some aspects of the methacrylic acid polymerization wave. The reaction zone (<1.2 mm) approximates a $\delta$ function and the polarizing $\mathbf{B}_0$ field does not greatly effect the front velocity. The induction period is not characterized by a homogeneous zone of reaction but appears to involve front propagation at a reduced, but variable, velocity. We conclude that NMRI can provide equivalent insight in to other polymerization reactions and, in particular, small-scale production or pilot plant polymerizations where the reaction proceeds inhomogeneously.

**Acknowledgment.** B.J.B. thanks NSERC of Canada for a postdoctoral fellowship; T.A.C. and L.D.H. thank Dr. Herchel Smith for a generous endowment. Andrew Derbyshire and Matthew Robson wrote the program to differentiate experimental profiles.

## References and Notes

(1) Callaghan, P. T. *Principles of Nuclear Magnetic Resonance Microscopy*; Oxford Science: Oxford, U.K. 1991.
(2) Listerud, J. M.; Sinton, S. W.; Drobny, G. P. *Anal. Chem.* **1989**, *61*, 23A–41A.
(3) Kuhn, W. *Angew. Chem., Int. Ed. Engl.* **1990**, *29*, 1–19.
(4) Attard, J. J.; Carpenter, T. A.; de Crespigny, A.; Duce, S. L.; Hall, L. D.; Hawkes, R. C.; Hodgson, R. J.; Herrod, N. J. *Phil. Trans. R. Soc. London, A* **1990**, *333*, 477–485.
(5) Jezzard, P.; Wiggins, C. J.; Carpenter, T. A.; Hall, L. D.; Jackson, P.; Claydon, N. J.; Walton, N. J. *Adv. Mater.* **1992**, *4*, 82–90.
(6) Pojman, J. A. *J. Am. Chem. Soc.* **1991**, *113*, 6284–6286.
(7) Gray, P. G.; Scott, S. K. *Chemical Oscillations and Non-Linear Chemical Kinetics*; Clarendon Press: Oxford, U.K. 1990.
(8) *Oscillations and Travelling Waves in Chemical Systems*; Field, R. J., Burger, M., Eds.; Wiley: New York, 1985.
(9) Zaikin, A. N.; Zhabotinskii, A. M. *Nature* **1970**, *225*, 535–537.
(10) Winfree, A. T. *Science* **1972**, *175*, 634–635.
(11) Field, R. J.; Noyes, R. M. *J. Am. Chem. Soc.* **1974**, *96*, 2001–2006.
(12) Lechleiter, J.; Girard, S.; Peralta, E.; Clapham, D. *Science* **1991**, *252*, 123–126.
(13) Winston, D.; Arora, M.; Maselko, J.; Gaspar, V.; Showalter, K. *Nature* **1991**, *351*, 132–135.
(14) Tzalmona, A.; Armstrong, R. L.; Menzinger, M.; Cross, A.; Lemaine, C. *Chem. Phys. Lett.* **1990**, *174*, 199–202.
(15) Weisenberger, L. A.; Koenig, J. L. *Macromolecules* **1990**, *23*, 2445–2453.
(16) Webb, A. G.; Hall, L. D. *Polymer* **1991**, *32*, 2926–2938.
(17) Balcom, B. J.; Carpenter, T. A.; Hall, L. D. *J. Chem. Soc., Chem. Commun.* **1992**, 312–313.
(18) Jackson, P.; Clayden, N. J.; Walton, N. J.; Carpenter, T. A.; Hall, L. D.; Jezzard, P. *Polym. Int.* **1991**, *24*, 139–143.
(19) Jezzard, P. Ph.D. Thesis, The University of Cambridge, 1991.
(20) Steiner, U. E.; Ulrich, T. *Chem. Rev.* **1989**, *89*, 51–147 and references therein.
(21) Hall, L. D.; Marcus, T.; Neale, B.; Powell, J.; Sallos, J.; Talagala, S. L. *J. Magn. Reson.* **1985**, *62*, 525–528.
(22) McConnell, J. *The Theory of Nuclear Magnetic Relaxation in Liquids*; Cambridge University Press: Cambridge, U.K., 1987.
(23) McCall, D. W. *Acc. Chem. Res.* **1971**, *4*, 223–232.
(24) McBrierty, V. J.; Douglas, D. C. *J. Polym. Sci., Macromol. Rev.* **1981**, *16*, 295–366.
(25) Gonzalez, R. C.; Wintz, P. *Digital Image Processing*; Addison-Wesley: London, 1977; p 155.
(26) McLauchlan, K. A.; Steiner, U. E. *Mol. Phys.* **1991**, *73*, 241–263.
(27) Young, R. J. *Introduction to Polymers*; Chapman and Hall: London, 1981; p 33.
(28) Russel, G. T.; Napper, D. H.; Gilbert, R. G. *Macromolecules* **1988**, *21*, 2141–2148.
(29) Reference 27, p 39.
(30) Calvin, P. In *Disorder and Mixing*; Guyon, E., Nadal, J. P., Pomeau, Y., Eds.; Kluwer Publishing: London, 1988; pp 293–315.
(31) Zeldovich, Y. B.; Barenblatt, G. I.; Librovich, V. B.; Makhviladze, G. M. *The Mathematical Theory of Combustion and Explosions*; Plenum; New York, 1985.
(32) Homas, S. W. *A Dictionary of Concepts in NMR*; Clarendon Press: Oxford, U.K., 1989; p 153.
(33) Reference 7, p 296.
(34) Henkelman, R. M.; Bronskill, M. J. *Rev. Magn. Reson. Med.* **1987**, *2*, 1–126.
(35) The presence of a small amount of monomeric acid will act as a plasticizer and depress $T_g$ to some extent.
(36) Quoted in: *Polymer Handbook*; Brandrup, J., Immergut, E. H., Eds. Wiley: New York, 1989; Chapter VI, p 218.